Journal of Renewable Materials

Tech Science Press

DOI: 10.32604/jrm.2023.023213

check for updates

ARTICLE

Evaluation of Novel Chitosan Based Composites Coating on Wettability for Pure Titanium Implants

Qahtan A. Hamad[1], Hanaa A. Al-Kaisy[1], Mohanad N. Al-Shroofy[1] and Noor K. Faheed[2,*]

[1]Materials Engineering Department, University of Technology, Baghdad, Iraq

[2]Petroleum Engineering Department, University of Misan, Amara, Iraq

[*]Corresponding Author: Noor K. Faheed. Email: noor.kf@uomisan.edu.iq

Received: 14 April 2022 Accepted: 10 June 2022

ABSTRACT

This work aims to prepare chitosan (CS)-based coated layers, CS (10 wt% nanosilver/90 wt% CS, 10 wt% biotin/90 wt% CS, and 5 wt% nanosilver–5 wt% biotin)/90 wt% CS coatings are prepared, onto pure Ti substrate. The surface morphology of the novel CS composite coating was studied using field emission scanning electron microscopy, atomic force microscopy (AFM), Fourier transforms infrared (FTIR) and wettability test. Results show that the addition of (biotin, nanosilver) 5 Vol.% improves the properties of composite materials. Using different particles' scale size aid in improving the combinations in the alginate, producing a dual effect on film properties. Coating surface roughness decreased in the chitosan-based biocomposite with preferable homogeneity and crack-free coating layers, as confirmed by AFM. An increase in surface roughness ensured substitution, which enhanced the surface structures. The high wettability of the CS-based coating layers was due to the presence of nanoparticles, and the composite coatings with CS, nanosilver, or biotin had excellent wettability because of the good hydrophilic nature of the CS matrix combined with reinforced particles. The FTIR results showed that peaks of the blending of CS plus nanoparticles, CS plus biotin, or CS plus nanosilver plus biotin were excellent matching with no changes in the structure of the matrix.

KEYWORDS

Nano silver; biotin; chitosan; coating; bio-composite; implants; titanium

1 Introduction

Biocompatibility is one of the basic requirements that should be met by metal biomaterial materials for medical applications, along with osseointegration, compatible mechanical properties, super corrosion, and erosion resistance [1,2]. Moreover, biomaterials should be nontoxic and should not induce inflammatory or hypersensitive reactions [3], given that they are extensively used in biotechnology, medicine, dentistry, and biotechnology. Most biomaterials comprise various types of materials as composite coatings with distinct atomic arrangements and varied structural, physical, chemical, and mechanical properties [4]. Metallic implants are susceptible to corrosion and the release of ions or wear of joints can cause serious infections and diseases [5]. The resistance of surgical bioimplants to corrosion is an essential feature because they are usually in direct contact with aggressive body fluids containing ions, such as chloride ions [6]. A metallic material is oxidized at anode sites, and dissolved oxygen is reduced to hydroxide

ions at cathode sites until a passive film forms on surfaces [7]. The modification of the metallic surface of the implant with biocomposite coating that stimulates the fixed and growth of bone cells is one way to increase the osseointegration and help stabilize the implant from any ions released or attacked by ion corrosion [2]. Furthermore, in recent years many studies to reduce the bacterial activity around the Ti implant focus on the coating of transpose components with biocompatible and antimicrobial coating materials added to the high dispersion stability [8]. In addition, surface modification (microstructures, nanostructures), differs from different improvements in biologically active coatings. Implants with improved biocompatibility, bioactivity, and antibacterial characteristics could be made by covering inorganic implants with biocompatible organic coatings [9]. For these well-certified benefits, such as in physiologically active coating, the use of bio coatings is one of the dominant approaches in biomedical fields to improve bone planting of Ti and Ti alloys (dental implants, for example) [10]. Biopolymers have identified themselves as a prospective group of substances with a wide variety of uses, the most notable of which being medicine. These materials are ideal candidates for implantable materials because of their biocompatibility, biodegradability, and lack of cytotoxicity [11]. Chitosan is a chitin-based biopolymer that is chemically similar to cellulose. Since it is non-toxic, biodegradable, and biocompatible, it is gaining popularity as a natural polymer. However, its surface area, particle size, and poor thermal and mechanical characteristics limit its manufacturing utilization [12]. The natural polymer chitosan (CS) is used with nanoparticles as a composite material to enhance antimicrobial biomaterial properties, such as biocompatibility and antimicrobial efficiency, for medical applications, including biodegradable materials, homeostasis, and drug delivery, skin transplantation, hemodialysis, and calcium absorption [13,14]. An in-house dip-coating approach was utilized by Noppakun et al. [15] to investigate the performance of (chitosan-copper) powder and composite coatings. The impacts of antimicrobial coatings on all composite coating layers raised the fraction of these particles, according to the findings. Field emission scanning electron microscopy (FESEM) and Fourier transform infrared (FTIR) spectroscopy were used to characterize and analyze the phases of raw material microstructures and deposition coatings.

In 2013, Jorge et al. [16] showed that the interactions of organic molecule 2-mercaptobenzothiazole (MBT) release corrosion inhibitors and polymer coating systems for the protection of (II) aluminum alloy AA2024. They were able to prepare the composite and used it as an “intelligent” pigment in a good barrier for high-performance applications. In 2017, Xu et al. studied the efficacy of the corrosion of the mild steel biotinic drug in 15% HCl acid with weight loss and electrochemical methods. Immersion time, temperature, activation energy, inhibitors, and concentration were studied. Polarization studies explored the mixed inhibitors of biotin. A surface study showed steel hydrophobicity with inhibitors prevents the formation of films on metallic surfaces with reduced corrosion rates [17]. In 2019, Tomasz et al. [18] studied the effect of substrate (TI6A4V) on the final characteristics of the coating. In addition, the air abrasion of air associated with corrosion is synergistic to produce a strong bond between peeking polymers (polyetheretherketone) and dental adhesives. In 2021, Isaa et al. [19] used the electrostatic deposition method to produce a thin poly (methyl methacrylate) compound coating layer from different bioceramics as reinforcing materials. The surfaces of the coating layers were homogeneous without cracking, and the mechanical properties improved.

The purpose of this study is to evaluate the wettability and other characteristics of chitosan (CS) based composite coating incorporating biotin and nanosilver as reinforcing materials that deposition on commercially pure Ti substrate through dip-coating method to form a biocomposite thin coating layer for enhancing and developing the surface properties of this metal. That is commonly used for implant devices replacing failed hard tissue, for example, artificial hip joints, artificial knee joints, bone plates, dental implants, and dental products, such as crowns and bridges.

2 Experimental Part

Commercially pure Titanium discs (Thommen Medical, Waldenburg, Switzerland; 2 mm × 1 mm × 1 mm) were used as substrates. The chemical composition of the Ti plate was as follows: Fe, 0.32%; O, 0.25%; N, 0.032%; C, 0.0075%; H, 0.014%; and Ti balance%. The surface of the substrate was mechanically molded to 80°, 100°, and 150° to increase the roughness of the surface through chemical composition analysis. Subsequently, the substrate was washed with deionized water and acetone and then dried before use. The dip-coating method was used in depositing a composite coating layer of CS-based composite with different reinforced materials, as shown in Table 1.

Table 1: Surface roughness and average diameter by AFM measurement

Sample No.	Composition of coating wt%
1	100% Pure chitosan
2	90% chitosan + 10% nanosilver
3	90% chitosan + 10% biotin
4	90% chitosan + 5% nanosilver + 5% biotin

The CS powder was dissolved in diluted acetic acid to give a milky solution for a pure CS coating sample. The solution is then placed on magnetic stirring to ensure the homogeneity of the solution and to eliminate existing bubbles presented, and the pH of the solution is measured. The pH value was increased to 6.0 by dropping the NaOH solution. Ti samples are dipped in the CS solution for 30 min, and then the samples are coated with a thin layer of composite coating (nanosilver and biotin) in solutions. The samples are coated with CS-based composite coating (CS + nanosilver, CS + biotin, or CS + nanosilver + biotin).

After deposition, the coated specimens dried again at room temperature, and samples were stored in polyester cans. The characterization of the composite coating specimens was examined by using the field emission scanning electron microscope (FESEM) and atomic force microscope. In addition, wettability tests were used, and the chemical bonding of composite coating was also determined by the Fourier transform infrared spectroscopy (FTIR).

3 Results and Discussion

3.1 Morphological Analysis (FESEM)

Fig. 1 displays the normal microstructure of CS composite coating samples became carried out with the use of Field emission scanning electron microscopy (FE-SEM). Images show complete surface observation of approximate samples, and illustrated the effect of particle addition (nanosilver and biotin) in CS matrix to the surface texture and homogeneously distributed on pure Ti substrate. The CS aggregate can be seen more clearly at high magnification (Fig. 1a). As shown in Figs. 1b and 1d, the CS-based composite coatings completely covered the Ti substrate. The surface was homogenous, and the addition of 5 wt%. nanosilver to CS resulted in a distinct morphology. The abnormal nature of the inorganic component and comparatively nonuniform distribution of nanoparticles within the CS matrix were found.

The microstructure images of polymer matrix with (5 wt%) biotin additions were examined. The surface coating texture was completely changed due to the biotin effect, surface roughness possibly decreased, and the homogeneity of the coating surface increased. These effects resulted in the clustering of components, such as nanosilver, within the coating structure and ultimately in the production of homogeneous coating layers. The addition of nanosilver and biotin resulted in a uniform and homogeneous finishing surface,

fine grain structure with excellent integration or embedded in the matrix and became part of it, so there is a uniform dispersion through the natural polymer matrix of the coating [20–22]. That is, no major cracks and porosity were observed within the CS matrix. In the top surface of samples of pure CS and CS with nanosilver and biotin, the porous surface promoted the interfacial bonding of the implant's surface with the surrounding medium, promoting osseointegration and enhancing the mechanical stability of implants.

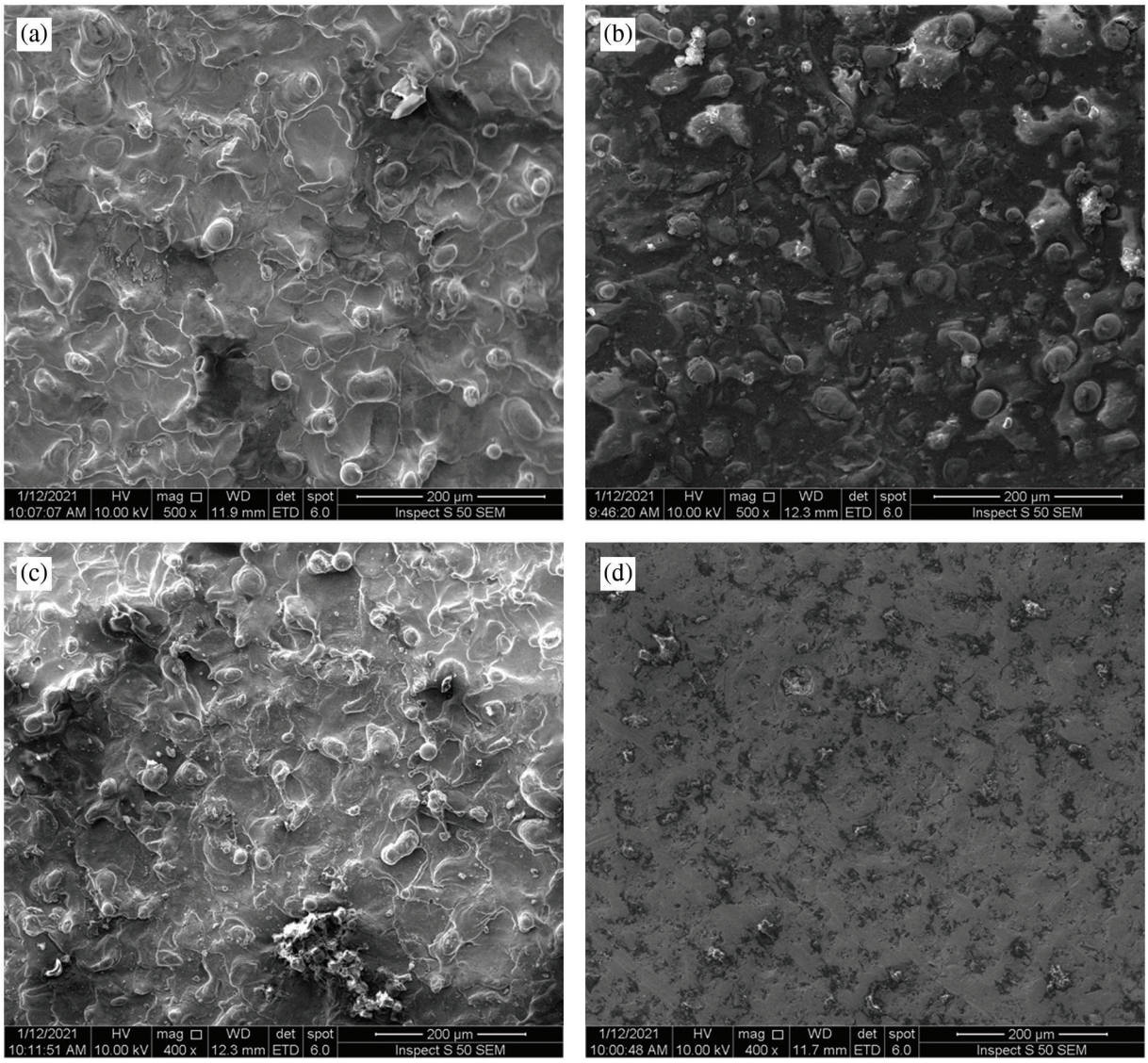

Figure 1: FESEM images of CS composite coated on pure Ti: (a) pure chitosan, (b) chitosan + Nanosiliver, (c) chitosan + biotin, and (d) chitosan + Nanosiliver + biotin

The composite coating thickness and average particle size were investigated through FESEM (Fig. 2). The coating thickness was approximately (33 nm), also, the average diameter of CS + nanosilver is approximately (332 nm) and (460 nm) of CS + biotin of the composite coated layer.

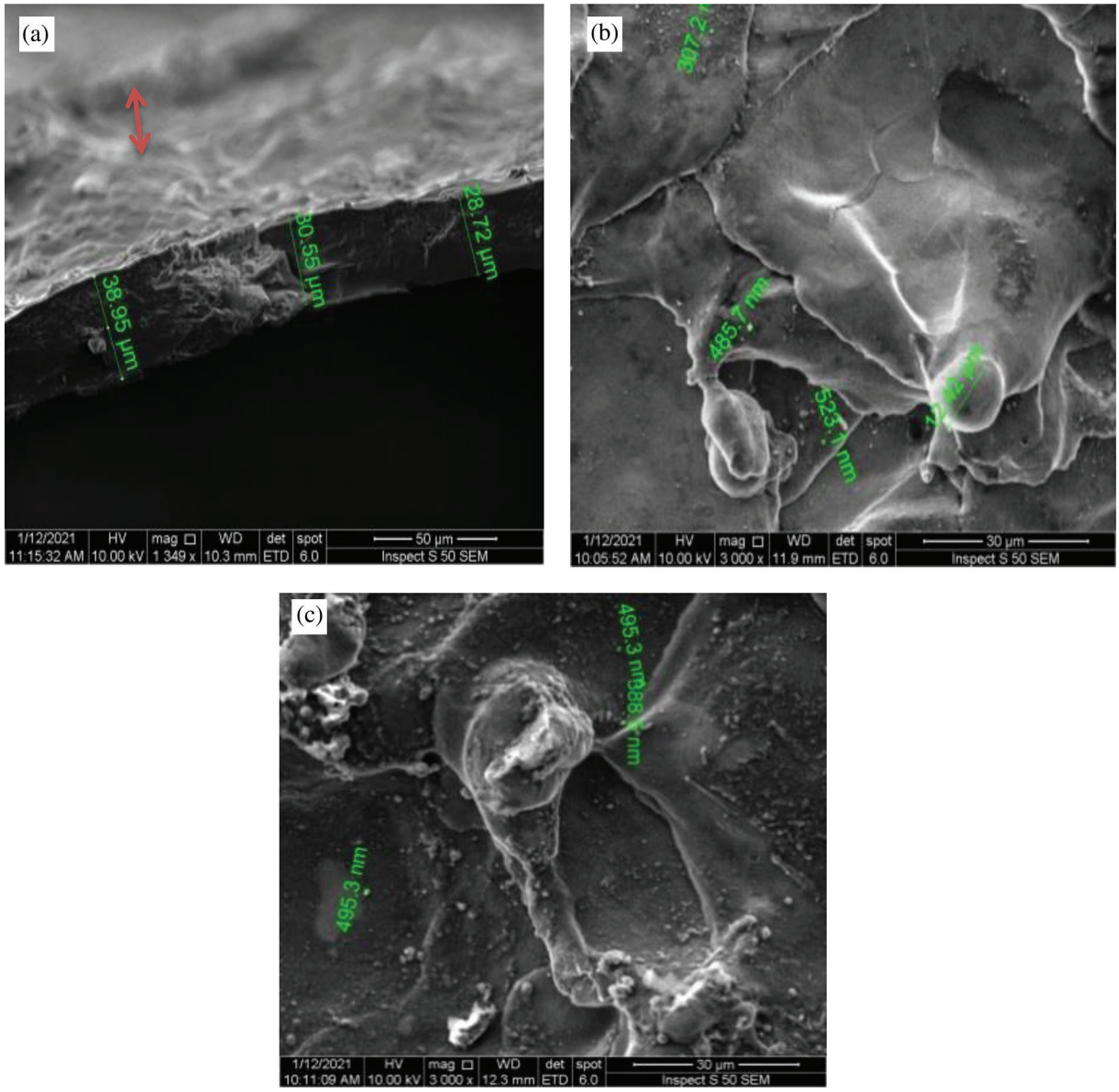

Figure 2: FESEM images of the (a) thickness of the coated layer, (b) average diameter of CS + nanosilver and (c) average diameter of CS + biotin of the composite coated layer

3.2 Surface Roughness

Fig. 3a shows the 2D and 3D topographic structures of pure CS-based coating specimens. Homogeneity and high roughness value were observed (8.89 nm with an average particle diameter of 94.28 nm), and the particle size distribution and surface topography of the CS coating were determined with an atomic force microscope. For the neat composite coating, the AFM result is illustrated in Figs. 3b–3d display the topographic structures with graphical distribution for (CS + nanosilver, CS + biotin, and CS + nanosilver + biotin) composite coating on a metal substrate. The composite-coated specimens showed coating layers with fine particles and homogenous surfaces because of the nanoparticles with biotin, which enhanced surface roughness and average diameter [23,24]. The coating layer was homogenous, and fine grains formed (Fig. 3d). Roughness and average particle diameters values for CS/nanosilver or biotin composite

coating samples were 5.65, 83.94, 4.94, and 80.42 nm, respectively, for CS/nanosilver or biotin composite coating, as shown in Table 2. The best value for improved coating was for the hybrid coating (CS/nanosilver/biotin) sample, which is 2.91 and 65.11 nm, respectively. The addition of both (biotin particles and nanosilver) presents very large changes in all surface coating properties making the coating surface roughness is decreased for CS base composite coating with preferable homogeneity which aids to enhance the surface structures (nano-roughness values) compared with pure CS coating (8.89 and 94.28 nm).

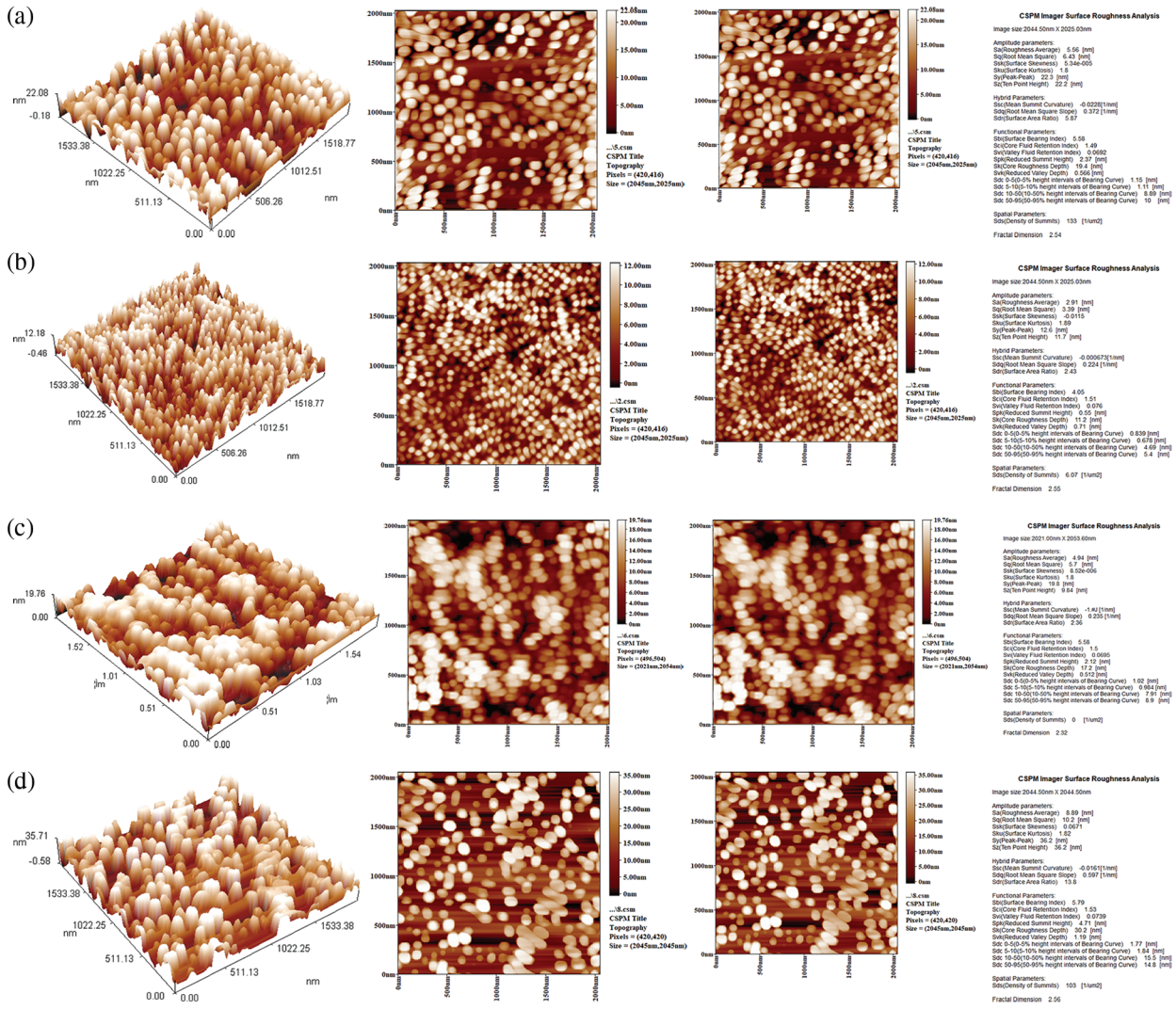

Figure 3: AFM image, 2D and 3D views for composite coating on 316L SS specimen (a) pure chitosan, (b) CS + Nanosiliver, (c) CS + biotin, and (d) CS + Nanosiliver + biotin

Table 2: Surface roughness and average diameter by AFM measurement

Type of substrate	Coating material (wt%)	Surface roughness (nm)	Ave. diameter (nm)
Pure Ti	Chitosan (CS)	8.89	94.28
	CS + nanosilver	5.65	83.94
	CS + Biotin	4.94	80.42
	CS + nanosilver + Biotin	2.91	65.11

3.3 Contact Angle Measurements

The contact angle is used to measure surface hydrophilicity at the moment of water droplet contact with the surface scaffold. It is more appropriate for part adhesion by evaluating how much a droplet of water could spread on a surface, and is an important feature known to have a significant influence on the biological responses to the implants. Nearly all of the studies have verified that surface hydrophilicity plays a crucial role in promoting the early stages of cellular migrations, proliferation, differentiation, and bone growth. Fig. 4 indicates the contact angle measurements of all the coated specimens compared with the substrate without coating after 30 s of depositing a drop of water over the surface of the sample. Fig. 4 depicts images of the pure chitosan sample's contact angle. The surface of this sample has a contact angle of roughly 78.64°, suggesting its hydrophilicity. Fig. 4 showed that the surface had a small water contact angle of approximately 63.32° for (chitosan + nanosilver + biotin) composite coating on Ti substrate because its surface particles minimized the contact angle of the hole composite coating materials and made the hydrophilic surface have a contact angle of 63.32°, as shown in Fig. 4. The addition of nanosilver at 5 wt% to the CS matrix minimized the contact angle to 69.63°, as shown in Fig. 4. The hydrophilicity of the surface decreased after the addition of biotin nanoparticles because of the increase in contact angle to 65.52°. This behavior was due to the reinforcement effect, which promoted mechanical interlocking between the polymer matrix and biotin. Particulate reinforcement reduced the roughness and enhanced surface homogeneity. Concerning the effect of CS concentrations on the contact angle, the contact angle decreased with adding the reinforcing materials into the CS matrix, indicating that the addition became increasingly hydrophilic because of the presence of active groups in CS, these active groups formed hydrogen bonds with water. The composites exhibit the same behavior with the addition of different proportions of the genipin crosslinking factor, because of the presence of functional groups and the genipin cross-linker is more hydrophilic than CS. In general, the contact angles for composite coating were small, indicating the high hydrophilicity of the coating layers [25–27]. The high wettability for CS-based composite coating layers was due to the presence of nanosilver particles and biotin as shown in Figs. 5a–5d. The coatings with (CS/nanosilver/biotin) composite coatings have the best wettability because of the excellent hydrophilic nature of the CS matrix combined with nanoparticles and biotin particles.

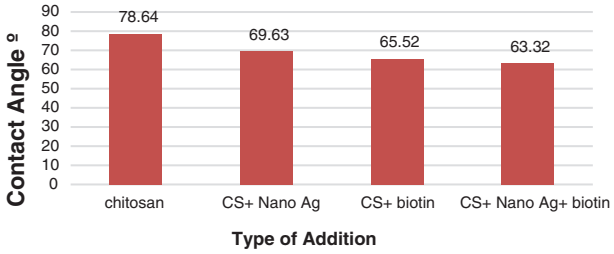

Figure 4: Contact angle results for CS-based composite coatings (nanosilver and biotin)

3.4 Fourier-Transform Infrared Spectroscopy (FTIR)

FTIR spectroscopy was used to identify the general formula, separate compounds, and determine the effective groups. The FTIR spectrophotometer of pure chitosan (CS) coating as illustrated in the plot (Fig. 6a) and CS-base composite coating that reinforcing by (nanosilver and biotin) in the plot (Figs. 6b–6d) appear with a broad peak around (600–3500 cm^{-1}). In a polymer study, Fourier Transform Infrared Resonance (FTIR) was used to classify polymers and visualize group ends as well as chain branching [13]. Because of the FTIR spectra of chitosan in Fig. 6a, the expansive band at 3253.33 cm^{-1} confirmed the gathers of amine and hydroxyl; 2358.98 cm^{-1} point was prompted by –CH strain; while the peak at 1743.62 cm^{-1}, it involved the vibrations of carbonyl (C=O). 1483.65 cm^{-1} point was ascribed to the stretching of N–H (ether and amide) and stretching of N–H (amide III bands). The structural tremor of

C–O was characterized by a 1013.59 cm^{-1} curve point while the [–CH2] and [–CH3] groups stretching vibration were assigned to the 2964.44 and 2927.55 cm^{-1} peaks, respectively [16].

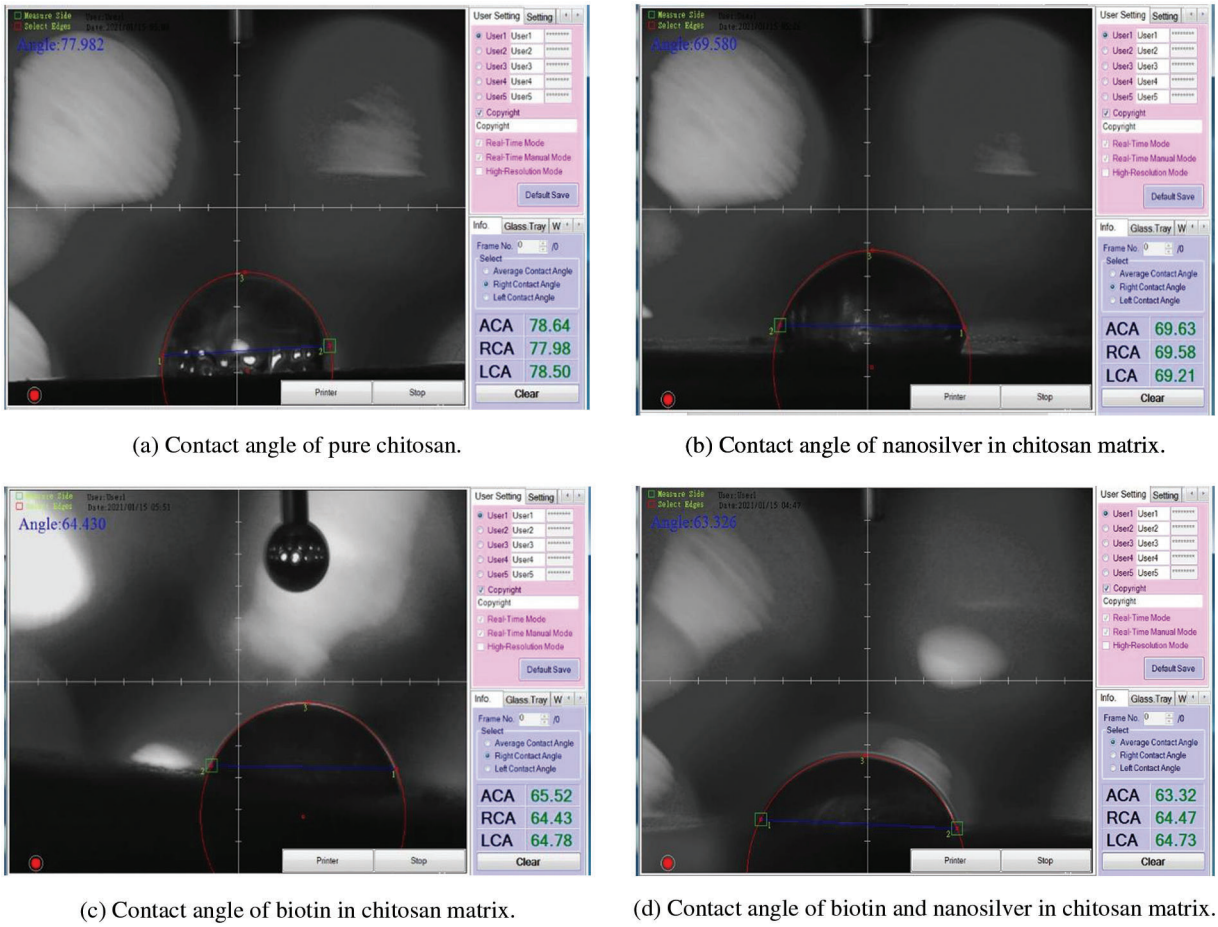

(a) Contact angle of pure chitosan.

(b) Contact angle of nanosilver in chitosan matrix.

(c) Contact angle of biotin in chitosan matrix.

(d) Contact angle of biotin and nanosilver in chitosan matrix.

Figure 5: (a) Contact angle of pure chitosan. (b) Contact angle of nanosilver in chitosan matrix. (c) Contact angle of biotin in chitosan matrix. (d) Contact angle of biotin and nanosilver in chitosan matrix

The same peak appeared in the FTIR spectra of the three coatings, composite coating (CS–nanosilver), (CS-biotin), and (CS–nanosilver–biotin). No differences were found among the spectra, and the composite coating showed no change in its structural polymer matrix, owing to coal interaction. But, these additions lead to a small increase in the peak intensity due to NH (amide II) to the 3244.22, 3251.38 and 3241.15 cm^{-1} as shown in Figs. 6b–6d. The absence of any chemical reaction between the composite components indicated an improved miscibility state and the absence of byproducts that might cause toxic and allergic effects inside the human body [19,28]. The reinforced CS with nanoparticles is in the vicinity of the peaks of 2359.75 and 2360.07 cm^{-1}, indicating that the OH group decreased in the polymer mixture (Figs. 6b and 6d). Given that the carboxylate group increased adhesion and ligation or interlocking between the coating layers, the composite coating can improve the biological activity of a commercially pure Ti. The same peaks appeared in the FTIR spectra of both coating groups and no change in the spectra of the polymer coating (CS–nanosilver–biotin) was observed. Furthermore, the composite coating showed no structural changes in its CS matrix [29,30].

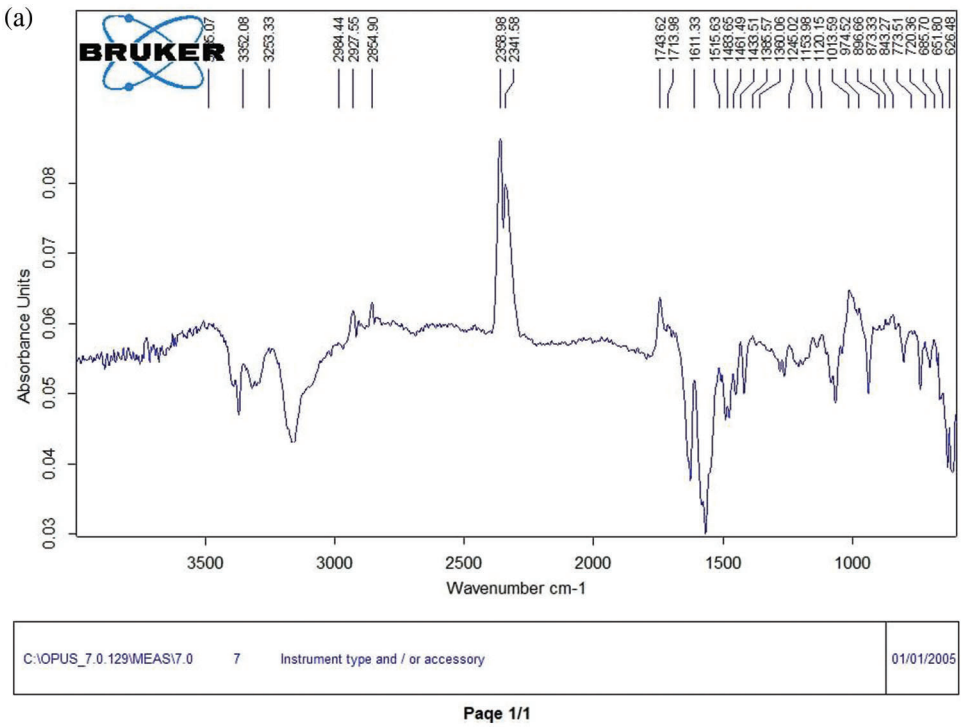

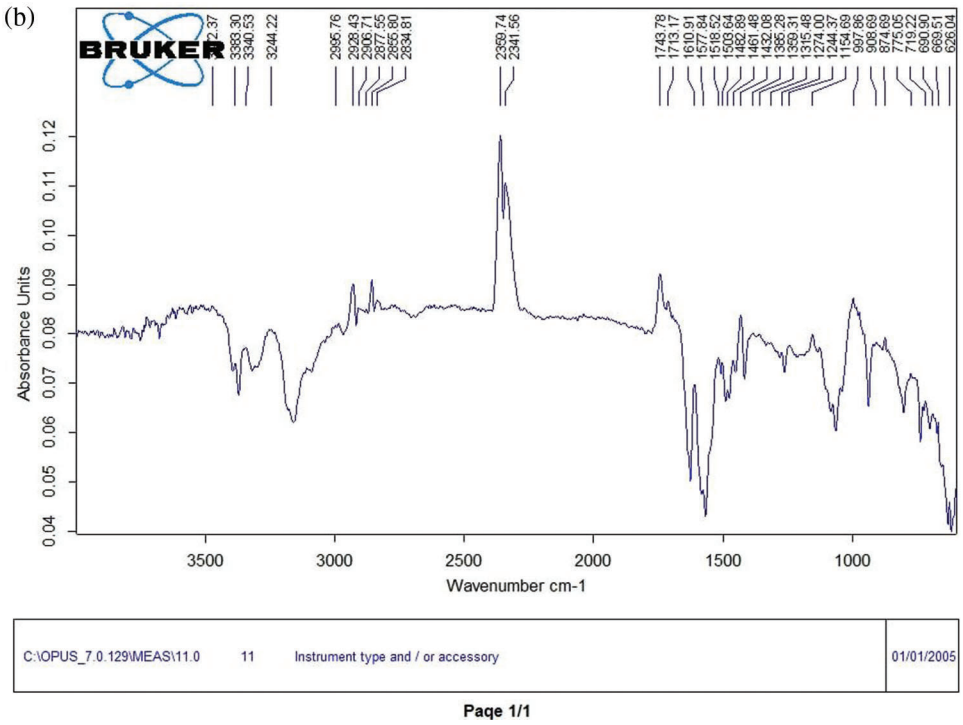

Figure 6: (Continued)

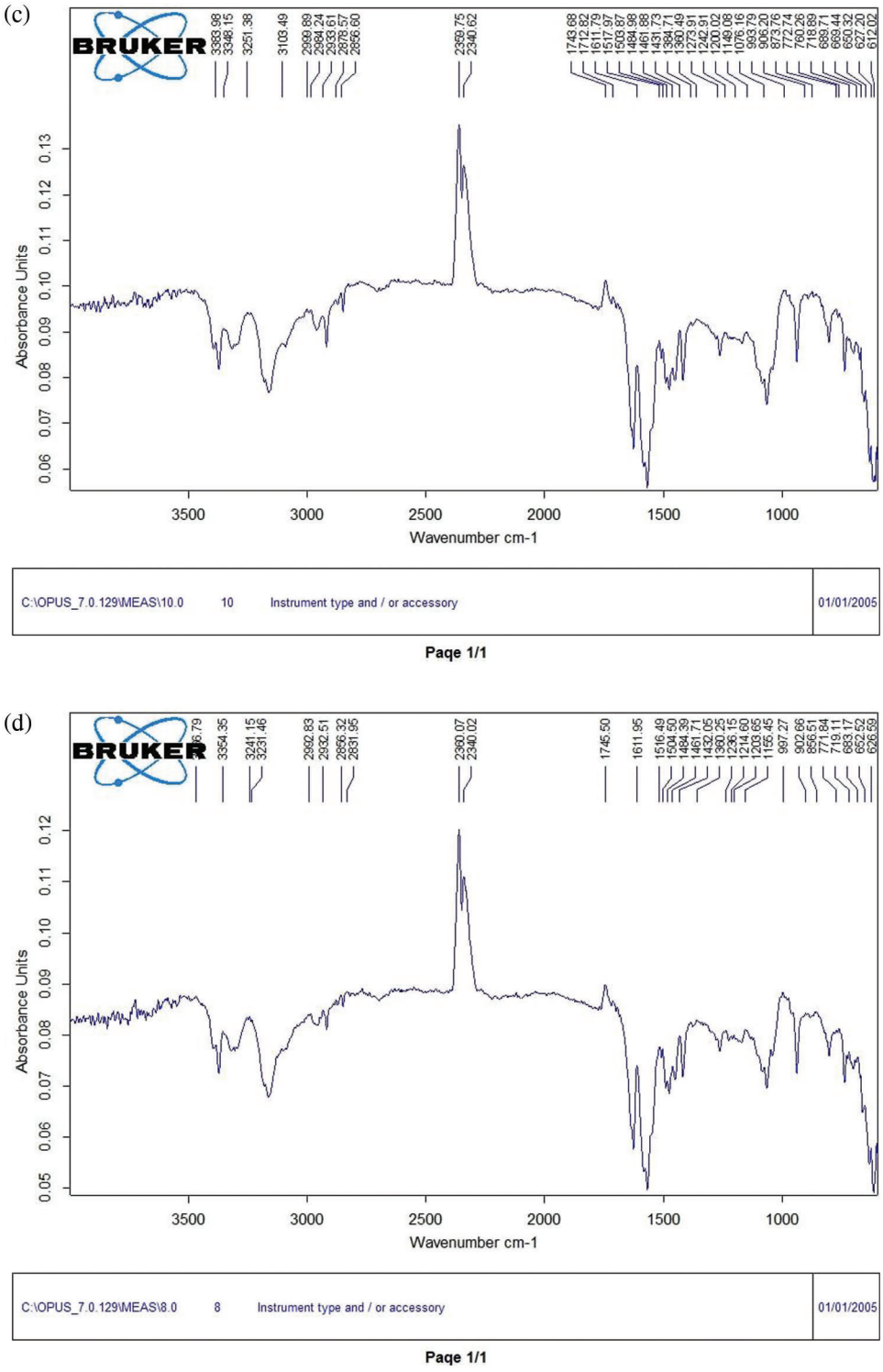

Figure 6: FTIR spectrum illustrate (a) pure chitosan coating, (b) CS + nanosilver, (c) CS + biotin and (d) CS + nanosilver + biotin composite coating

4 Conclusions

The dip-coating deposition technique may be used in synthesizing CS-based composite coating reinforced with nanosilver and biotin. The SEM images indicated homogeneous adhesion between the coating layer and the Ti substrate, confirming the suitability of the coating technique. Moreover, nanosilver and biotin precipitated in the CS polymer matrix, promoting dispersion in the composite coating surface, increasing density, resulting in inhomogeneity, and enhancing adhesion. The composite coating thickness and average particle size obtained through FESEM were 30 nm, and the average diameter was approximately 332.1 nm.

The addition of biotin and nanosilver particles changed the surface coating properties. These changes include coating surface roughness decreased in the composite coating layers, which showed desirable homogeneity in the distribution of biotin and nanosilver particles in the chitosan (CS) matrix, which have roughness and average diameter values (2.91 and 65.11 nm), respectively, compared with pure CS coating layers (8.89 and 94.28 nm), respectively. While FTIR results showed the same peak appears in the FTIR spectra of the composites coating groups (CS–nanosilver–biotin) compared with pure CS coating. Also, no obvious difference in the spectra and no change in the structure of polymer matrix composite coating for composite coating was observed.

Acknowledgement: The authors would like to express thanks to all the staff at the Faculty of Engineering at the University of Technology–Baghdad.

Funding Statement: The authors received no specific funding for this study.

Conflicts of Interest: The authors declare that they have no conflicts of interest to report regarding the present study.

References

1. Manivasagam, G., Dhinasekaran, D., Rajamanickam, A. (2010). Biomedical implants, corrosion and its prevention–A review surface modification of Ti alloys by plasma cleaning to enhance antibacterial activity: Corrosion and its prevention–A review. *Recent Patents on Corrosion Science, 2,* 40–54. DOI 10.2174/1877610801002010040.
2. Santos, G. (2007). The importance of metallic materials as biomaterials. *Advances in Tissue Engineering & Regenerative Medicine: Open Access, 3(1),* 00054.
3. Joseph, D. R. P., Bronzino, D. (2015). *Biomedical engineering fundamentals*. 4th edition. London, New York: CRC Press.
4. Asri, R. I. M., Harun, W. S. W., Samykano, M., Lah, N. A. C., Ghani, S. A. C. et al. (2017). Corrosion and surface modification on biocompatible metals: A review. *Materials Science and Engineering: C, 77,* 1261–1274. DOI 10.1016/j.msec.2017.04.102.
5. Bosco, R., van den Beucken, J., Leeuwenburgh, S., Jansen, J. (2012). Surface engineering for bone implants: A trend from passive to active surfaces. *Coatings, 2(3),* 95–119. DOI 10.3390/coatings2030095.
6. Doe, Y., Ida, H., Seiryu, M., Deguchi, T., Takeshita, N. et al. (2020). Titanium surface treatment by calcium modification with acid-etching promotes osteogenic activity and stability of dental implants. *Materialia, 12,* 100801. DOI 10.1016/j.mtla.2020.100801.
7. Li, B., Xia, X., Guo, M., Jiang, Y., Li, Y. et al. (2019). Biological and antibacterial properties of the micro-nano structured hydroxyapatite/chitosan coating on titanium. *Scientific Reports, 9(1),* 1–10.
8. Hendriks, J., van Horn, J. R., van der Mei, H. C., Busscher, H. (2004). Backgrounds of antibiotic-loaded bone cement and prosthesis-related infection. *Biomaterials, 25(3),* 545–556. DOI 10.1016/S0142-9612(03)00554-4.
9. Wang, Z., Zhitomirsky, I. (2022). Deposition of organic-inorganic nanocomposite coatings for biomedical applications. *Solid, 3(2),* 271–281. DOI 10.3390/solids3020019.

10. Jiang, T., Zhang, Z., Zhou, Y., Liu, Y., Wang, Z. et al. (2010). Surface functionalization of titanium with chitosan/gelatin via electrophoretic deposition: Characterization and cell behavior. *Biomacromolecules, 11,* 1254–1260. DOI 10.1021/bm100050d.
11. Rita, R., Margarida, F., Fangueiroa, R. (2017). Biopolymers in medical implants: A brief review. *Procedia Engineering, 200,* 236–243.
12. Gebregiorgis Ambaye, T., Mentore, V., Shiv, P., Hullebusch, E., Rtimi, S. (2022). Preparation and applications of chitosan and cellulose composite materials. *Journal of Environmental Management, 301,* 113850.
13. Wei, D., Sun, W., Qian, W., Ye, Y., Ma, X. (2009). The synthesis of chitosan-based silver nanoparticles and their antibacterial activity. *Carbohydrate Research, 344(17),* 2375–2382.
14. Raafat, D., Sahl, H. G. (2009). Chitosan and its antimicrobial potential, a critical literature survey. *Microbial Biotechnology, 2(2),* 186–201.
15. Noppakun, S., Siao, M. A., Philip, C., Khor, K. A. (2009). Antibacterial property of cold sprayed chitosan-Cu/A'll coating. *Journal of Thermal Spray Technology, 18(4),* 600–608.
16. Jorge, C., Joao, T., Susana, C. M. F., Carmen, S. R., Alessandro, G. et al. (2013). Chitosan as a smart coating for controlled release of corrosion inhibitor 2-mercaptobenzothiazole. *ECS Electrochemistry Letters, 2(6),* 19–22.
17. Xu, X., Singh, A., Sun, Z., Ansari, K. R., Lin, Y. (2017). Theoretical, thermodynamic and electrochemical analysis of biotin drug as an impending corrosion inhibitor for mild steel in 15% hydrochloric acid. *Royal Society Open Science, 4(12),* 1–17.
18. Tomasz, M., Maciej, W., Sławomir, Z., Alicja, L. (2019). Improvement of the Ti-6Al-4V alloy's tribological properties and electrochemical corrosion resistance by nanocomposite TiN/PEEK708 coatings. *Metallurgical and Materials Transactions A, 50(12),* 1–11.
19. Isaa, R. A., Al-Shroofy, M. N., Al-Kaisy, H. A. (2021). Al_2O_3-TiO_2-PMMA bio-composite coating via electrostatic spray technique. *Engineering and Technology Journal, 39(3A),* 504–511.
20. Kadhim, N. N., Hamad, Q. A., Oleiwi, J. K. (2020). Tensile and morphological properties of PMMA composite reinforced by pistachio shell powder used in denture applications. *AIP Conference Proceedings, 2213(1),* 020078.
21. Algailani, H. M., Mahmoud, A. K., Al-Kaisy, H. A. (2020). Fabrication of Ni-ZrO_2 nanocomposite coating by electroless deposition technique. *Engineering and Technology Journal, 38(5),* 649–655. DOI 10.30684/etj.v38i5A.491.
22. Aljumaily, M. M., Alayan, H. M., Mohammed, A. A., Alsaadi, M. A., Alsalhy, Q. F. et al. (2022). The influence of coating super-hydrophobic carbon nanomaterials on the performance of membrane distillation. *Applied Water Science, 12(28),* 1–8. DOI 10.1007/s13201-021-01564-5.
23. Faheed, N. K., Oleiwi, J. K., Hamad, Q. H. (2021). Effect of different fiber reinforcements on some properties of prosthetic socket. *Engineering and Technology Journal, 39(11),* 1715–1726. DOI 10.30684/etj.v39i11.2267.
24. Al-Ani, F. H., Alsalhy, Q. F., Raheem, R. S., Rashid, K. T., Figoli, A. (2020). Experimental investigation of the effect of implanting TiO_2-NPs on PVC for long-term UF membrane performance to treat refinery wastewater. *Membranes, 10(77),* 1–22. DOI 10.3390/membranes10040077.
25. Valeria, C., Ettore, P., Giovanni, V., Gianluca, C., Arti, A. et al. (2008). Genipin-crosslinked chitosan/gelatin blends for biomedical applications. *Journal of Materials Science: Materials in Medicine, 19,* 889–898.
26. Lin, Z., Wang, Y., Wang, D., Zhao, B., Chang, L. J. (2013). Porous structure preparation and wettability control on titanium implant. *Surface and Coatings Technology, 228,* 131–136. DOI 10.1016/j.surfcoat.2012.07.007.
27. Aljumaily, M. M. (2020). Superhydrophobic nanocarbon-based membrane with antibacterial characteristics. *Biotechnology Progress, 36(3),* 1–13. DOI 10.1002/btpr.2963.
28. Oleiwi, J. K., Hamad, Q. A., Abdulrahman, S. A. (2022). Comparative study of polymeric laminated composites reinforced by different fibers of prosthetic socket by DSC and FTIR. *Key Engineering Materials, 911,* 3–8. DOI 10.4028/p-ju39wm.
29. Halla, M., Alzuhairi, M., Sarmad, I. I., Saif, H. S. (2021). Ternary waste plastic blends for binding and adhesion. *International Journal of Environmental Studies, 78(6),* 897–1069.
30. Zahraa, H. A., Zaidoon, S. M., Alzuhairi, M., Farooq, A. S. (2021). Thermal and catalytic cracking of plastic waste: A review. *International Journal of Environmental Analytical Chemistry, 78(3),* 363–536.